MONITORING OF WINTER WHEAT SEEDLING AT JOINTING STAGE USING REMOTE SENSING TECHNIQUES

CHANGWEI TAN*, DUNLIANG WANG, MING LUO, YING DU, JIAN ZHOU,
WEIWEI YAN AND YONGJIAN ZHANG

*Jiangsu Key Laboratory of Crop Genetics and Physiology/Co-Innovation Center for Modern
Production Technology of Grain Crops, Yangzhou University, Yangzhou 225009, China*

Abstract

A quantitative correlation between major seedling condition parameters in winter wheat at the jointing stage and the grain quality parameters, production, and remote sensing variables was conducted. It is possible to predict leaf area index, SPAD value and leaf nitrogen content in winter wheat at the jointing stage by normalized difference vegetation index (NDVI), and to predict biomass using near-infrared band reflectance (B_4), respectively. The remote sensing models of the leaf area index, SPAD value, leaf nitrogen content and biomass of winter wheat were credible, and higher precision with determination coefficient (R^2) of 0.709, 0.701, 0.671 and 0.612, respectively, and with root mean square error (RMSE) of 0.641, 3.499, 0.347% and 486.3 kg/hm^2, respectively. Spatial distribution map of the major seedling condition parameters of winter wheat could be implemented at different classes with remote sensing method.

Introduction

The growth and production of winter wheat are closely related to the quality of the grain, and major parameters including the LAI, biomass, SPAD value, and LNC. One of the tasks of remote sensing is to monitor agriculture and the growth of plants and level of growth at different stages.

Over the past years, the different remote sensing data and methods have been used to monitor crop growth; consequently plenty of valuable information was obtained (Kyu-Sung *et al.* 2004, Tan *et al.* 2005, Gnyp *et al.* 2014, Bsaibes *et al.* 2009). Date back to the early 1980s, the vegetation indices curve extracted from LANDSAT MSS and NOAA had been used to assess the growth of crops (Crist and Malila 1980, Schneider *et al.* 1981, Moriondo *et al.* 2007). The vegetation indices had been used to assess the growth of crops in order to survey the impacts of disaster (Tappan *et al.* 1990). Hunt *et al.* (2013) found that the triangular greenness index (TGI) was related to leaf chlorophyll content. Timely detection of growth parameters of crop with remote sensing technology on a regional scale is important to ascertain canopy energy exchange in agro-ecosystems (Li *et al.* 2014, Delegido *et al.* 2013). Focuses are now concentrated on the possibility of retrieving rice plant parameter such as plant age, height, biomass etc. (Ozdogan and Gutman 2008). Airborne hyperspectral remote sensing was applied to analyze the nitrogen content in rice at panicle initiation stage by using data of three years (Chanseok *et al.* 2010).

It is important to note that China had launched the A and B satellites (called HJ-1A/1B) of "Environment and Disaster Monitoring and Forecasting Small Satellite Constellation System" with independent intellectual property rights on September 6, 2008. These satellites have CCD sensors with broad band, 30 m spatial resolution, and 2-day-time resolution by parallel observation. This provides an ideal data source for the industrialization of agricultural remote sensing monitoring.

---

*Author for correspondence: <tanwei010@126.com>. Agricultural College, Yangzhou University, 48 Wenhui Road (E), Yangzhou 225009, Jiangsu Province, P. R. China.

There exists a system of remote sensing monitoring of the growth of crops, however, the system need to be improved. The generality of farm management service is poor and studies on the mechanisms are insufficient (Tan *et al.* 2011). For winter wheat especially, research on the major growth parameters at the jointing stage is unclear, plus the precision and accuracy of remote sensing monitoring do not satisfy the production. More studies are necessary to improve the quality and reliability of remote sensing.

This study made use of the remote sensing data of the HJ-1A/1B satellites to monitor the LAI, biomass, SPAD value, and LNC of winter wheat at the jointing stage, assess the growth, display the spatial distribution of the growth parameters, select the sensitive variables of remote sensing for the monitoring of the major growth parameters, build and verify the models based on the sensitive variables of the major growth parameters. The obtained data could offer global information for the assessment of fertilization and irrigation and improve the quality and production in winter wheat crops.

Materials and Methods

Experiment 1: There were a total of 60 samples, made up of 10 - 20 samples acquired from XingHua, DaFeng, TaiXing and JiangYan counties in Jiangsu Province, China in 2012. The geographic location of each sample was obtained by Juno ST portable GPS (Trimble, USA). The investigation indicators included winter wheat varieties, growth stages, group growth, and disasters (primarily pests). The winter wheat varieties included Yangmai No. 13, Yangmai No. 15, Yangmai No. 16, Yangfumai No. 2, and Ningmai No. 9. The sampling periods included the jointing and ripening stages. The exact sampling periods depended on the satellite passing time and the experimental areas. Typically, for each experimental field, plants with similar growing trends were selected in areas of four rows by 50 cm, the length measured with rulers, and the location recorded by GPS at the time. After sampling, LAI (lamina mass per unit area method), biomass (weighing method), SPAD value (SPAD-502 detecting), LNC (Kjeldahl method), and the parameters of the quality of the winter wheat at the ripening stage (acquired by near infrared instrument for crop quality detection), including the content of protein were tested in a laboratory. The satellite data were derived from the passing images of the HJ-1A/1B satellites on March 23 at the jointing stage. The data were used as the testing samples of the assessment models.

Experiment 2: There was a total of 60 samples, made up of 10 - 20 samples from GaoYou, Xing Hua, Tai Xing and Jiang Yan counties in Jiangsu Province in 2013. The other conditions were the same as Experiment 1. The data were derived from the satellite passing images of the HJ-1A/1B satellites on March 27 at the jointing stage. The data were used as the testing samples of the assessment models.

Experiment 3: There was a total of 120 samples, 30 samples acquired from Xing Hua, Da Feng, JiangYan, Tai Xing, and Yi Zheng counties in Jiangsu Province in 2014, with the other conditions similar to Experiment 1. The data were derived from the satellite passing images of the HJ-1A/1B satellites on March 25 at the jointing stage. The data were used as the training samples of the building models.

Study areas located in the center of Jiangsu Province (119°12′to 120°26′East longitude & 32°2′ to 33°16′North latitude), is one of the main winter wheat production areas in Jiangsu. The areas have subtropical moist monsoon climate, dish-shaped plain depression, about 1000 mm annual average precipitation, and about 2200 hrs annual average sunshine. In the experimental area, wheat seeds were sown in November of the first year and harvested in June of second year. In this research, the samples were harvested at jointing stage in the month of March, which is the key period of wheat plant growth process.

The data used in this study were derived from images provided by the HJ-1A/1B satellites from China center of resources satellite data and application. The images had high spatial resolution and spectral resolution including blue, green, red, and near infrared spectral bands.

The preprocessing of the images was conducted with ENVI. Firstly, geometric corrections of the images were conducted based on the topographic maps (scale 1 : 100 000) of Jiangsu province, China. Then, further geometric corrections were conducted based on the GPS control points on the ground. The atmospheric radiometric corrections and the conversions of reflectivity were conducted by the empirical linear method (Tan *et al.* 2011).

The variables of the satellite remote sensing were calculated using Excel, based on the brightness values of the GPS sampling points extracted by ENVI5.1, ArcGIS10.2, and the existing satellite remote sensing spectral indices algorithms. Based on the data from Experiment 3, the correlations between the major growth parameters of winter wheat at the jointing stage and the variables of the satellite remote sensing were analyzed, and a remote sensing monitoring model was built by regression and optimization through goodness of fit (R^2). The model was assessed based on the data of Experiments 1 and 2, R^2, and root mean square error (RMSE) (Tan *et al.* 2011). A list of common multi-spectral satellite remote sensing vegetation indices is presented in Table 1.

Table 1. Some common multi-spectral satellite remote sensing vegetation indices.

Vegetation index	Calculation formulas	Sources
Difference vegetation index (DVI)	$= B_4 - B_3$	Jordan (1969)
Ratio vegetation index (RVI)	$= B_4/B_3$	Jacobsen (1998)
Normalized difference vegetation index (NDVI)	$= (B_4 - B_3)/(B_4 + B_3)$	Serrano *et al.* (2000)
Green normalized difference vegetation index (GNDVI)	$= (B_4 - B_2)/(B_4 + B_2)$	Daughtry *et al.* (2000)
Plant senescence reflectance index (PSRI)	$= (B_3 - B_1)/B_4$	Sims and Gamon (2002)
Structure intensive pigment index (SIPI)	$= (B_4 - B_1)/(B_4 + B_1)$	Penuelas *et al.* (1995)
Nitrogen reflectance index (NRI)	$= (B_2 - B_3)/(B_2 + B_3)$	Schleicher *et al.* (1981)
Soil adjusted vegetation index (SAVI)	$= (B_4 - B_3)/(B_4 + B_3 + 0.5)*(1 + 0.5)$	Huete and Jackson (1988)
Optimal soil adjusted vegetation index (OSAVI)	$= (1 + 0.16)* (B_4 - B_3)/(B_4 + B_3 + 0.16)$	Rondeaux *et al.* (1996)

B_1, B_2, B_3 and B_4 denoted spectrum reflectance of HJ-1A/1B images at blue, green, red and near infrared bands, respectively.

Results and Discussion

Table 2 shows the correlations between major growth parameters of winter wheat and the quality and production. The results from Experiment 3 showed that, at the jointing stage, the LNC was significantly correlated with the SPAD value and the starch content, while the SPAD value was significantly correlated with the protein, wet gluten, and starch content. The biomass was found to significantly correlate with the LAI and the starch, protein and wet gluten content.

Table 3 shows the correlation between major growth parameters and the variables of remote sensing. It showed that at the jointing stage, the SPAD value had a significant correlation with B_3, B_4, NDVI, NRI, GNDVI, SIPI, PSRI, DVI, RVI, SAVI and OSAVI. The correlation with NDVI was significant, with a correlation coefficient of 0.837. According to the rule of sensitive parameter determination (Valérie *et al.* 2008), NDVI is the best variable used to invert the SPAD value and

could provide information for the decision of winter wheat cultivation. It was also found that biomass was significantly correlated with B_4, NDVI, NRI, SIPI, PSRI, DVI, RVI, SAVI, and OSAVI. The correlation with B_4 was the strongest ($r = 0.782$, $p < 0.01$), which means B_4 is the best variable used to invert the biomass. The LAI was significantly correlated with B_2, B_3, NDVI and NRI; the correlation with NDVI was the strongest ($r = 0.842$, $p < 0.01$), which means NDVI is the optimal variable used to invert the LAI. The LNC was significantly correlated with B_3, B_4, NDVI, GNDVI, SIPI, PSRI, DVI, RVI, SAVI, and OSAVI. The correlation with NDVI was the strongest ($r = 0.819$, $p < 0.01$) which means NDVI is the best variable used to invert the LNC. In summary, it is possible to invert the SPAD value, biomass, LAI, and LNC with the remote sensing variables of NDVI, B_4, NDVI, and NDVI.

Table 2. Correlation between growth parameters, grain quality and yield (n = 120).

	LAI	LNC (%)	SPAD	Biomass (kg/hm^2)	Yield (kg/hm^2)	GPC (%)	WGC (%)	GSC (%)
LAI	1.000							
LNC (%)	0.085	1.000						
SPAD	0.014	0.566**	1.000					
Biomass (kg/hm^2)	0.652**	0.173	0.148	1.000				
Yield (kg/hm^2)	–0.119	–0.133	0.078	-0.17	1.000			
GPC (%)	–0.002	–0.172	–0.247*	-0.303*	–0.173	1.000		
WGC (%)	0.016	–0.117	–0.253*	-0.254*	–0.120	0.919**	1.000	
GSC (%)	0.030	0.240*	0.271*	0.385**	0.270*	–0.563**	–0.556**	1.000

*Significant at $p < 0.05$, **Significant at $p < 0.01$, n: Total samples number.

Table 3. Correlation coefficients between key growth indices and multi-spectral remote sensing variables (n = 120).

	LAI	LNC (%)	SPAD	Biomass (kg/hm^2)
B_1	0.091	–0.080	0.054	–0.070
B_2	0.431**	–0.008	0.082	–0.070
B_3	0.704**	–0.294*	–0.433**	–0.209
B_4	0.215	0.613**	0.618**	**0.782****
NDVI	**0.842****	**0.819****	**0.837****	0.437**
NRI	0.258*	0.135	0.327*	0.553**
GNDVI	–0.020	0.537**	0.508**	0.140
SIPI	0.162	0.621**	0.564**	0.315*
PSRI	–0.087	–0.495**	–0.687**	0.392**
DVI	0.180	0.656**	0.687**	0.382**
RVI	0.159	0.651**	0.696**	–0.275*
SAVI	0.140	0.676**	0.720**	0.437**
OSAVI	0.140	0.676**	0.720**	0.437**

*Significant at $p < 0.05$, **Significant at $p < 0.01$, n: Total samples number.

Based on the aforementioned results, the remote sensing variables of the major growth parameters were selected based on their correlations. The remote sensing monitoring models of the major growth parameters were built through linear regression using the sensitive remote sensing variables as the dependent variables and the growth parameters as the independent variables. The final remote sensing monitoring model of the major growth parameters at the jointing stage was identified by the determining coefficient with highest R^2 (Fig. 1).
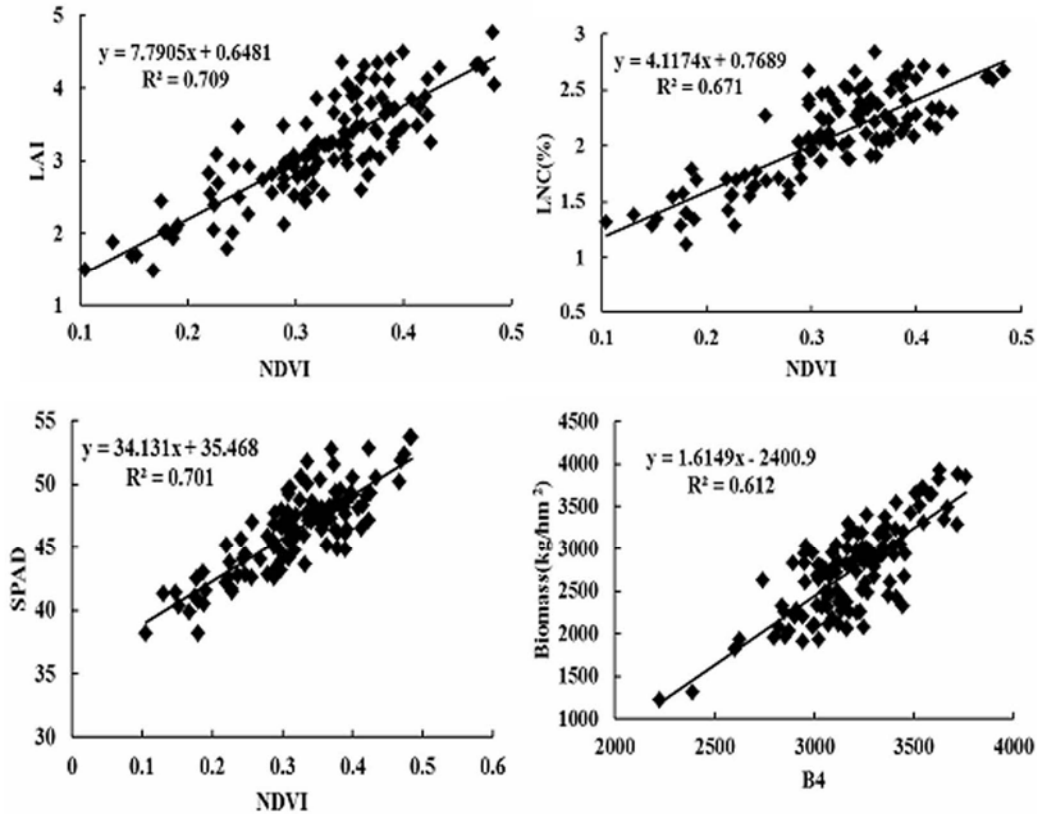
Fig.1. Remote sensing models for monitoring growth status parameters of winter wheat.

The reliability of the models was assessed by the relationship model (Fig. 1) and regression analysis of the predicted values and observed values (Fig. 2), R^2, and RMSE value based on the data of 2012 and 2013 (Table 4). The results showed that the correlation between the predicted values and observed values were significant, and the R^2 and RMSE were ideal. This indicated that the models are capable of monitoring the major growth parameters with higher accuracy (Fig. 2), especially for using the NDVI to monitor the SPAD with the highest R^2 and RMSE, which were 0.85 and 2.67, respectively. Additionally, according to the results shown in Table 2, it is possible to use these models to indirectly calculate other agronomic parameters related to these major growth parameters.
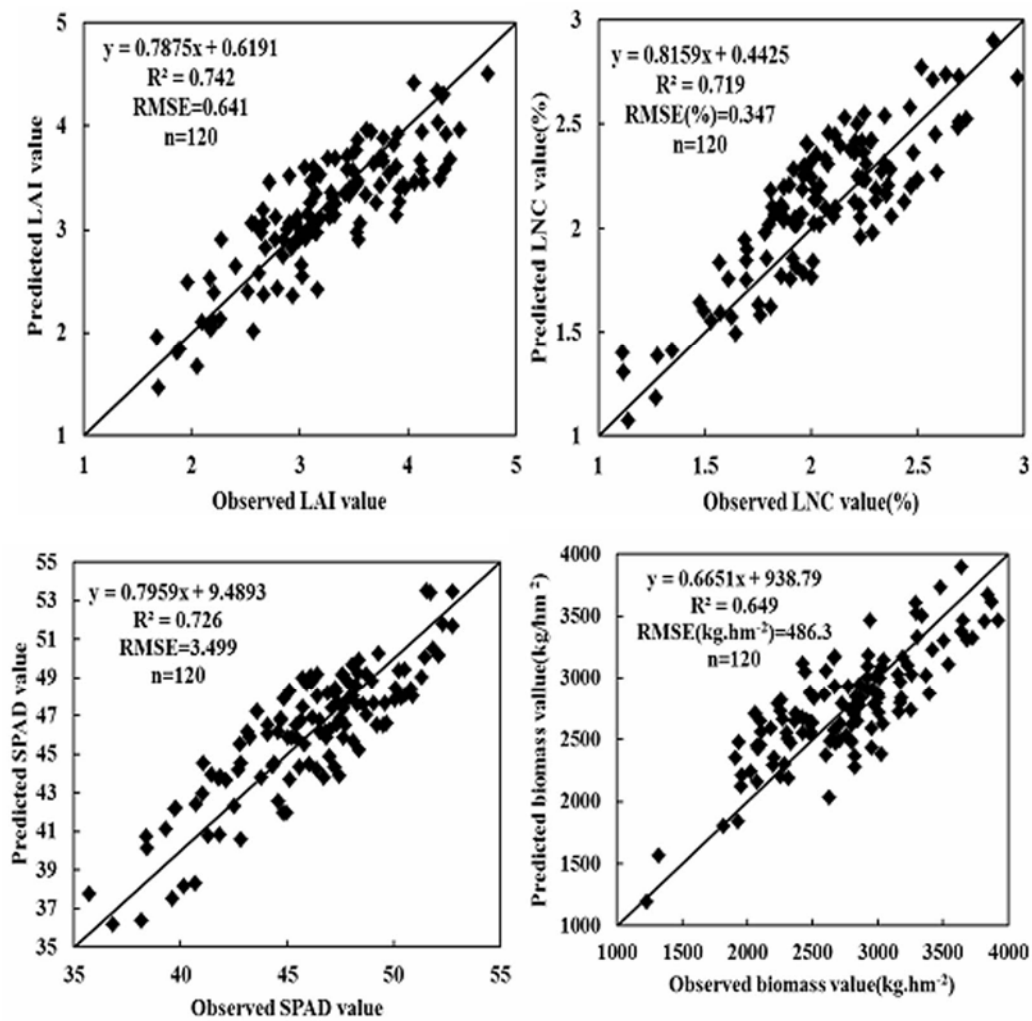
Fig. 2. Evaluating the remote sensing models for monitoring growth status parameters of winter wheat.

Table 4. Results of evaluating the remote sensing monitoring models.

Growth stage	Independent variables (x)	Dependent variables (y)	Models	R^2	RMSE
	NDVI	LAI	y = 7.7905x + 0.6481	0.742**	0.641
Jointing stage	NDVI	LNC (%)	y = 4.1174x + 0.7689	0.719**	0.347
	NDVI	SPAD	y = 34.131x + 35.468	0.726**	3.499
	B_4	Biomass (kg/hm^2)	y = 1.6149x – 2400.9	0.649**	486.3
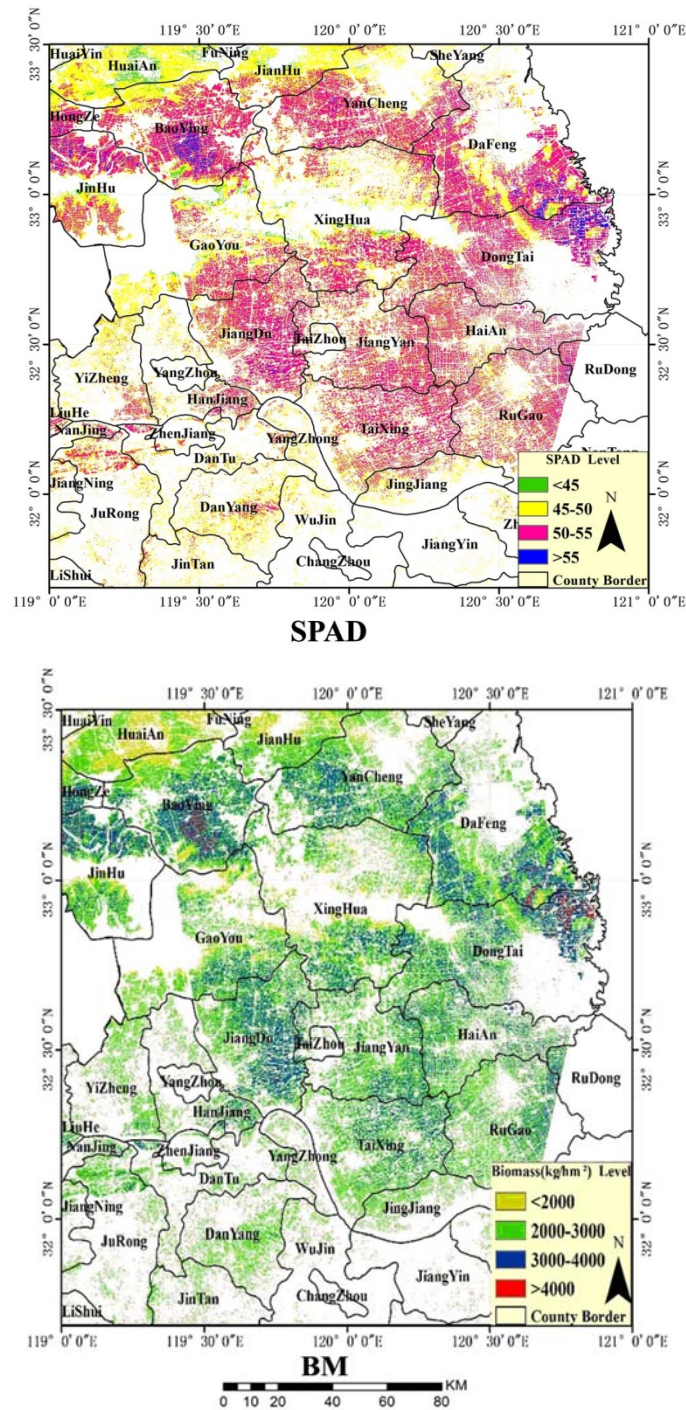
Fig. 3. Thematic maps for monitoring growth parameters (SPAD & BM) of winter wheat.
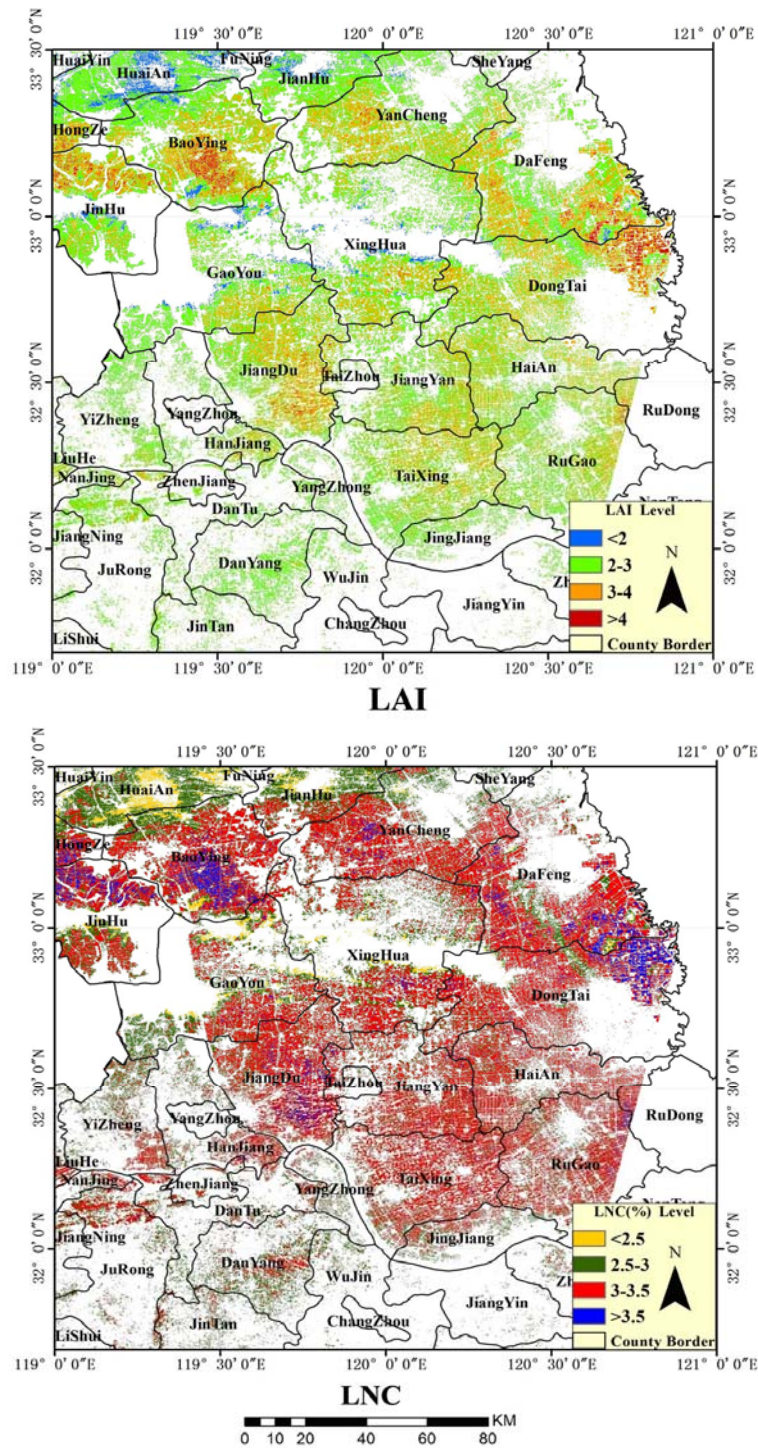
Fig. 4. Thematic maps for monitoring growth parameters (LAI & LNC) of winter wheat.

Thematic maps were made on the basis of SPAD value, biomass, LAI, and LNC of winter wheat using the remote sensing variables (Figs 3-4). Non-planted areas were removed by binary mask overlay with wheat planting distribution data and vector data of administrative boundary (Fig. 3). LAI values are shown as 3 - 4 or higher than 4 and most of the LNC (%) values are 3.0 - 3.5, 2.5 - 3.0 in the northern area of JianHu and higher than 3.5 in the Jin Hu, BaoYing, Da Feng and Dong Tai areas (Fig. 4). Most of the SPAD values are higher than 50, with values higher than 55 in the Bao Ying and Dong Tai areas, 45-50 in the northern area of Jian Hu, and lower than 45 in some areas of Huai An (Fig. 3). Fig. 2 also shows that the biomass (kg/hm^2) is higher than 4000 in the Bao Ying, Da Feng and Dong Tai areas, 2000 - 3000 and 3000 - 4000 in the most areas covered by images, and lower than 2000 in some areas of Jian Hu. These results were consistent with field investigations and information provided by local agricultural departments as well.

The main findings were: (1) It is possible to invert the LAI, LNC, SPAD value, and biomass in wheat growth by remote sensing variables. (2) Remote sensing monitoring models were built for LAI, LNC, SPAD, and biomass. Moreover, the model accuracy was also verified. (3) The spatial distribution of the growth parameters could be implemented by remote sensing monitoring thematic maps of the LAI, LNC, SPAD value, and biomass of winter wheat at the jointing stage at different levels.

Acknowledgements

References

Bsaibes A, Courault D, Baret F, Weiss M and Olioso A 2009. Albedo and LAI estimates from FORMOSAT-2 data for crop monitoring. Remote Sens. Environ. **113**(4):716-729.

Chanseok R, Suguri M and Umeda M 2010. Model for predicting the nitrogen content of rice at panicle initiation stage using data from airborne hyperspectral remote sensing. Biosyst. Eng. **104**(4): 465-475.

Crist E P, Malila W A. 1980. Temporal-spectral analysis of technique of vegetation applications of landsat. *Proceedings of the 14th Symposium on Reomte Sensing of Environment*, held at San Jose, Costa Rica, 23-30 April.

Daughtry CST, Walthall CL, Kim MS, Colstoun EBD and Iii MM 2000. Estimating Corn Leaf Chlorophyll Concentration from Leaf and Canopy Reflectance. Remote Sens. Environ. **74**(2): 229-239.

Delegido J, Verrelst J, Meza CM, Rivera JP, Alonso L and Moreno J 2013. A red-edge spectral index for remote sensing estimation of green LAI over agroecosystems. Eur. J. Agron. **46**: 42-52.

Gnyp ML, Miao Y, Yuan F, Ustin SL, Yu K, Yao YK, Huang SY and Bareth G 2014. Hyperspectral canopy sensing of paddy rice aboveground biomass at different growth stages. Field Crops Res. **155**: 42-55.

Huete AR and Jackson RD 1988. Soil and atmosphere influences on the spectra of partial canopies. Remote Sens. Environ. **25**(1):89-105.

Hunt E R, Doraiswamy PC, Mcmurtrey JE, Daughtry CST and Perry EM 2013. A visible band index for remote sensing leaf chlorophyll content at the canopy scale. Int. J. Appl. Earth Obs. **21**(1): 103-112.

Jacobsen, Stephen C 1998. Sensor system for determining acceleration. Dumont Et Al.

Jordan CF 1969. Derivation of Leaf Area Index from Quality of Light on the Forest Floor. Ecology **50**(4): 663-666.

Kyu-Sung L, Warren B Cohen, Robert E Kennedy and Thomas K 2004. Maiersperpger, Stith T. Gower. Hyperspectral versus multispectral data for estimating leaf area index in four different biomes. Remote Sens. Environ. **91**(1): 508-520.

Li F, Mistele B, Hu Y, Chen X and Schmidhalter U 2014. Reflectance estimation of canopy nitrogen content in winter wheat using optimised hyperspectral spectral indices and partial least squares regression. Eur. J. Agron. **52**(1): 198-209.

Moriondo M, Maselli F and Bindi M 2007. A simple model of regional wheat yield based on NDVI data. Eur. J. Agron. **26**(3): 266-274.

Ozdogan M and Gutman G 2008. A new methodology to map irrigated areas using multi-temporal MODIS and ancillary data: An application example in the continental US. Remote Sens. Environ. **112**(9): 3520-3537.

Penuelas J, Baret F and Filella I 1995. Semiempirical Indexes to Assess Carotenoids Chlorophyll-a Ratio from Leaf Spectral Reflectance. Photosynthetica **31**(2):221-230.

Rondeaux G, Steven M and Baret F 1996. Optimization of soil-adjusted vegetation indices. Remote Sens. Environ. **55**(2): 95-107.

Schneider SR, Mcginnis DF and Gatlin JA 1981. Use of NOAA AVHRR visible and near-infrared data for land remote sensing. NOAA Technical Report NASS84, USDA, Washington, D, C.

Serrano L, Ustin SL, Roberts DA, Gamon JA and Peñuelas J 2000. Deriving Water Content of Chaparral Vegetation from AVIRIS Data. Remote Sens. Environ.**74**(3): 570-581.

Sims DA and Gamon JA 2002. Relationships between leaf pigment content and spectral reflectance across a wide range of species, leaf structures and developmental stages. Remote Sens. Environ. **81**(2-3): 337-354.

Tan CW, Wang JH, Huang YD, Huang WJ and Liu LY 2005. Quantitative improvement of Beer-Lambert law with spectral remote sensing technology and its application. Scientia Agr. Sinica **38**(3): 498-503. (in Chinese with English abstract)

Tan CW, Wang JH, Zhao CJ, Wang Y, Wang JC, Tong L, Zhu XK and Guo WS 2011. Monitoring wheat main growth parameters at anthesis stage by Landsat TM. Transactions of the CSAE **27**(5): 224-230. (in Chinese with English abstract)

Tappan GG, Moore DB and Howard SM 1990. The design and operational use of AVHRR vegetation index image for crop protection in AFRICA. Presented at Twenty-Third International Symposium on Remote Sensing of Environment. Bangkok, Thailand.

Valérie D, Sylvie D, Frédéric B, Marie W and Gérard D 2008. Estimation of leaf area and clumping indexes of crops with hemispherical photographs. Agr. & Forest Meteorol. **148**(4): 644-655.